Supplementary Materials

1. NFS spectra of (**1**)

In order to check the thermal behaviour of the obtained title complex the 95% 57-Fe enriched sample of [Fe(trzH)$_2$(trz)](BF$_4$), prepared according to ref. 9 (modification 1a) was measured with nuclear forward scattering (NFS)[i] in heating and cooling mode in the 340-400 K area. The results are shown in Figure 1. The complex in heating mode shows typical NFS spectrum of low-spin Fe(II) with no beating (low quadrupole splitting) at 340 and 360K. At 400K the NFS signal practically disappears most probably due to a very low Lamb Mössbauer factor. Upon cooling back to 360K the spectrum reveals typical high-spin iron (II) pattern with beating. This behaviour corresponds to cooperative behaviour reported for the [^{57}Fe(trzH)$_2$(trz)](BF$_4$)] system (ref. 9), that displays the hysteretic transition with T_c=385K ↑ and T=345K ↓, with bistability region between ca. 350 and 390 K

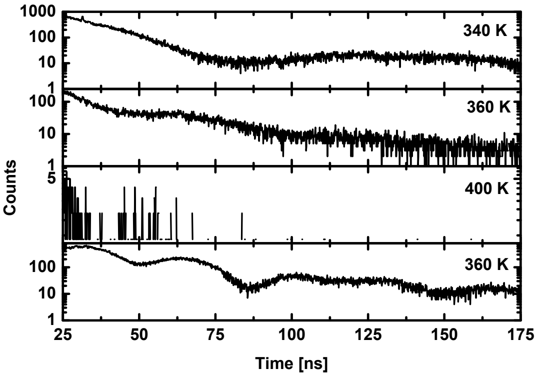

Figure 1S. NFS spectra of [^{57}Fe(trzH)$_2$(trz)](BF$_4$)] at 340, 360 and 400K in heating mode (top three) and at 360K in cooling mode (bottom).

2. NIS spectra of HS (**1**)

In order to obtain the pDOS of [^{57}Fe(trzH)$_2$(trz)](BF$_4$) in the HS state NIS measurements were performed at 360 K in cooling mode (after heating to 400 K). Three NIS energy scans have been measured, one scan taking ca. 50 minutes. The results of each scan are shown in Figure S2.

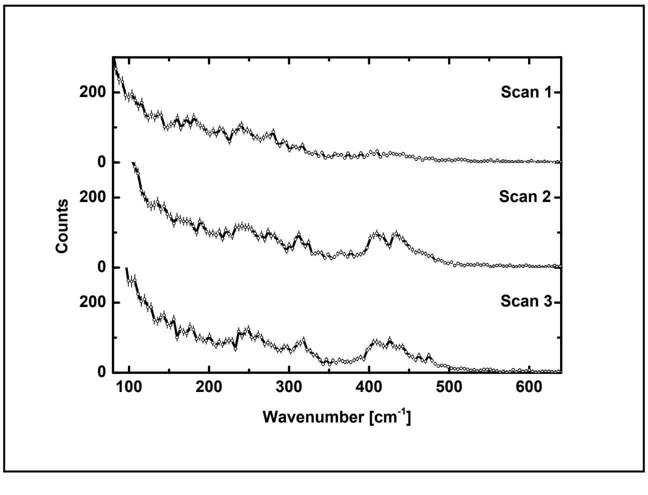

Fig. 2S NIS spectra of three subsequent scans of [^{57}Fe(trzH)$_2$(trz)](BF$_4$) at 360K in cooling mode.

The first scan (Fig. S2, top) taken after cooling down to 360 K shows only a weak shoulder occuring in the LS marker band area. The two further scans reveal a partial recovery of the LS state with progressing time. As expected, the signals due to the HS isomer appear essentially below 300 cm^{-1}.

In order to extract the experimental pDOS of the HS state from the NIS data shown in Figure S2, we have calculated the pDOS from the spectrum as obtained after the first scan (Figure S2, top). Subsequently the pDOS of the LS state obtained at 80 K was subtracted, assuming a molar LS fraction of the latter to be 0.25 for the sample. The so obtained pDOS is shown in Figure S3 .

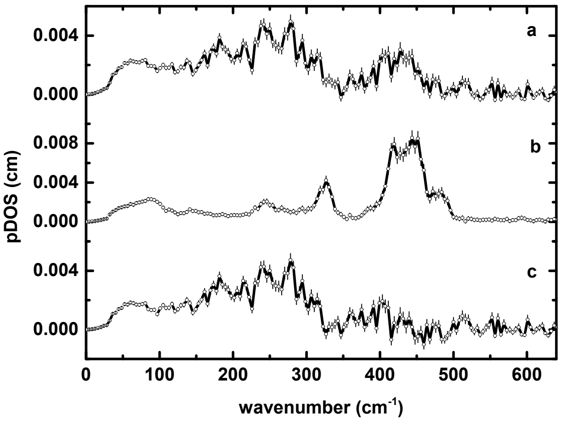

Fig. 3S: a**)** pDOS of [^{57}Fe(trzH)$_2$(trz)](BF$_4$) at 360 K in cooling mode as obtained from the first NIS scan (Fig. 2a). b) pDOS of the LS state obtained from NIS data taken at 80 K. c) pDOS of the HS state as obtained by subtracting the pDOS of the LS state assuming a LS contribution of 25 %.

3. Spin transition in (**2**)

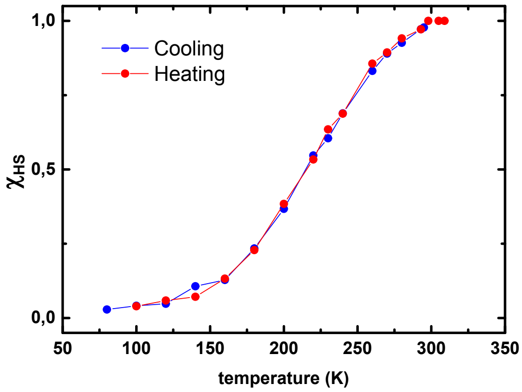

Figure S4. Temperature dependence of the high-spin fraction in the diluted sample (**2**) in cooling and heating mode. The high-spin fraction was determined with conventional Mössbauer spectroscopy.

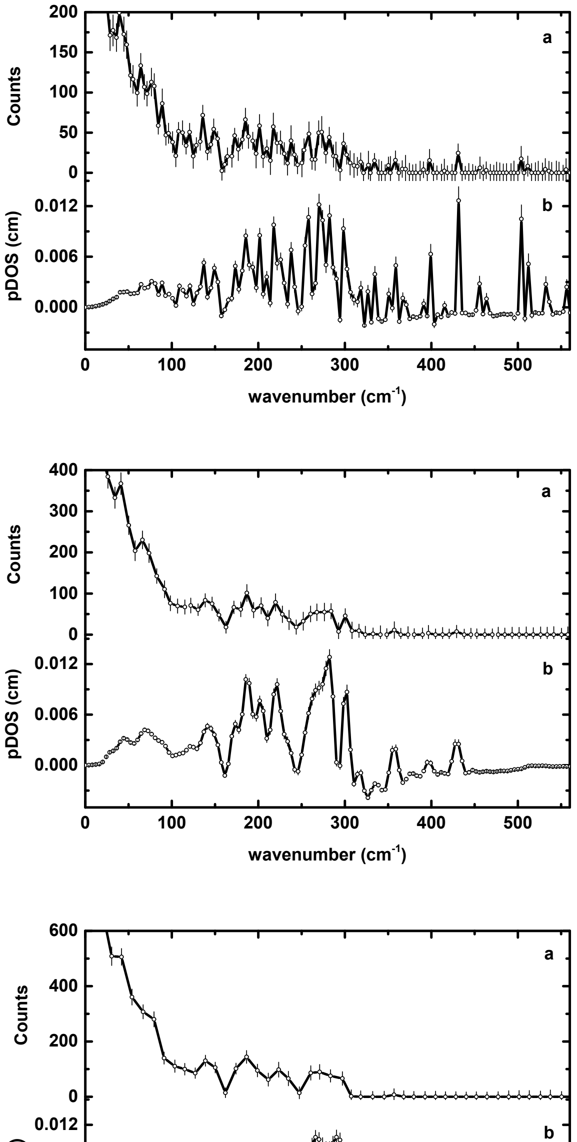

Fig. S5. NIS spectra of the diluted sample (**2**) at room temperature (a) with the pDOS (b) for different binnings (0.5, 1 and 1.5 meV, top, middle and bottom, respectively). A constant background was subtracted from the spectra.

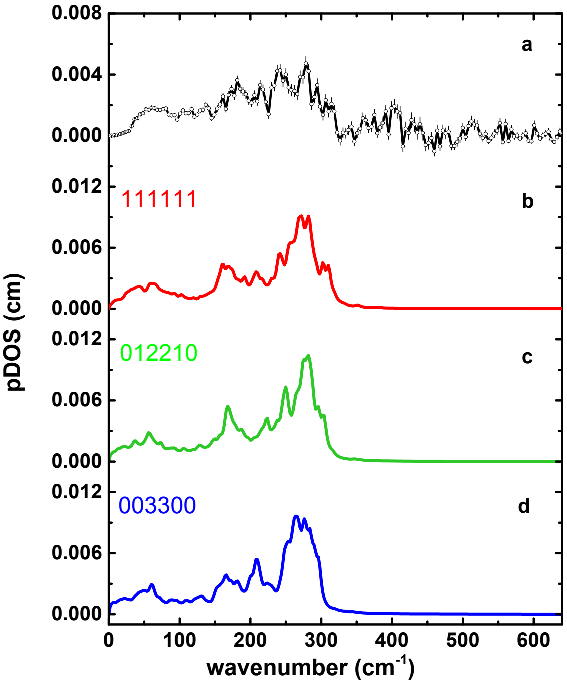

Fig. S6: Experimental pDOS of the high-spin state of (**1**) (a) and the simulated pDOS (b)-(d)of the heptameric model HHHHHHH with the three different anion models.

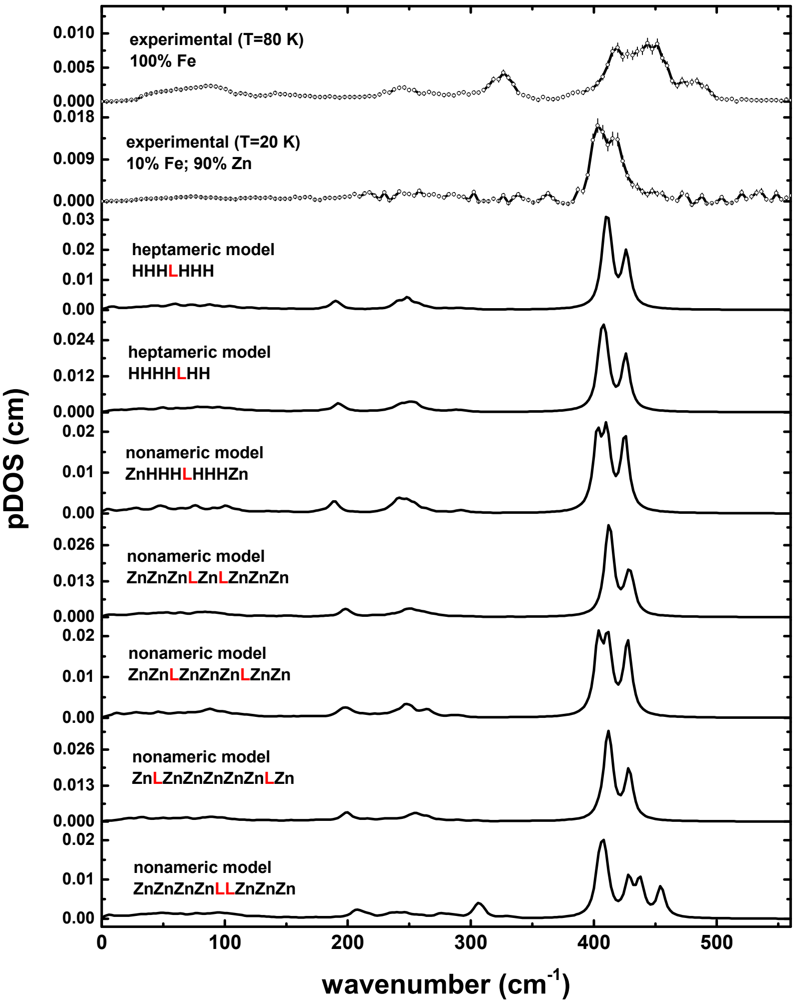

Fig. S7: Comparison of experimental pDOS of (**1**) (a) and the diluted sample (2) (**b**) with different models of spin isomers containing LS centre as a minor component (c–i). The shown simulated pDOS represent the density of states of the particular red marked iron centres (L=low-spin iron, H=high-spin iron, Zn= zinc).

MO orbitals of the model of 1D polyazole Fe(II) complexes.

The ideal symmetry of a homoleptic $[Fe(azole)_3X_2]_n$ linear 1D polynuclear chain is S_6. Therefore, the d-orbitals of iron are of a_g (d_z2) and e_g type. The latter have the complex representation in this cyclic group and hence the pairs of d_{yz}, d_{xz} and d_{xy}, $d_x2_{-y}2$, being of e_g type have different energies. In order to show the shapes and orientation of the d-orbitals in the above complexes, we present the results of the DFT calculation for the fully LS trimeric molecule of $[(H_2O)_3Fe(atrz)_3Fe(atrz)_3Fe(OH_2)_3]Cl_6$[17], for which the S_6 symmetry was assumed. The obtained d-orbital of the central Fe atom, revealing the S_6 environment are shown in Figures 6S and 7S. The first conclusion is that the S_6 axis, identical to the long axis of the chain defines the z-coordinate. The d_z2 orbital a_g lies at the lowest energy and is clearly a non-bonding one. The two further occupied d-orbitals, the first two e_g ones, are also of non-bonding character, they combine only with the p-orbitals of chlorine anion. Interestingly, their mutual orientation displays that they are related by a rotation at 45 deg along the z-axis (see Figure 8S). Thus, they may be described as d_{xy}, and , $d_x2_{-y}2$ orbitals. Note that the plane of none of them is perpendicular to z-axis. On the other hand the two virtual d-orbitals

(d_{xz} and d_{yz}) clearly form the σ-bonds with the p-orbitals of the aminotriazole ligands. It is noteworthy that one of them (178) displays a typical contour of the d-orbitals other than the d_z2 one, while the 179 one shows a different shape, somewhat closer to the d_z2 orbital (see Fig. 6S).The former forms a bond with four N atoms, the latter with two. Actually, they correspond to the e_g orbitals in the coordinates of the Fe-N_6 octahedron (for further perspective views see Figure S9). The unique assigning the of the x- and y-axis of the orbital systems of the molecular system may be achieved the following way: the x-axis lies in the plane of two *trans* coordinated azole ligands so that the y one lies in the plane defined by four remaining coordinated nitrogen atoms (see Fig. 12 in the main text).

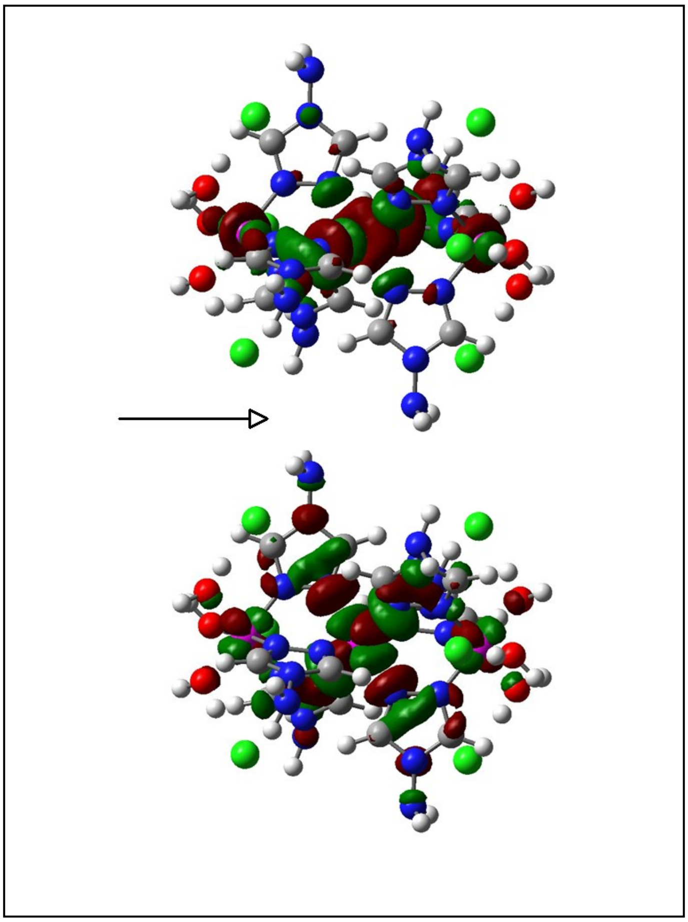

Fig. S8**:** Virtual MO orbitals (178, bottom and 179, top) of predominantly d-character for central Fe atom in S_6 isomer of LS (all three irons) of $[(H_2O)_3Fe(atrz)_3Fe(atrz)_3Fe(OH_2)_3]Cl_6$. The molecule is shown with its S_6 axis orientation given by the arrow.

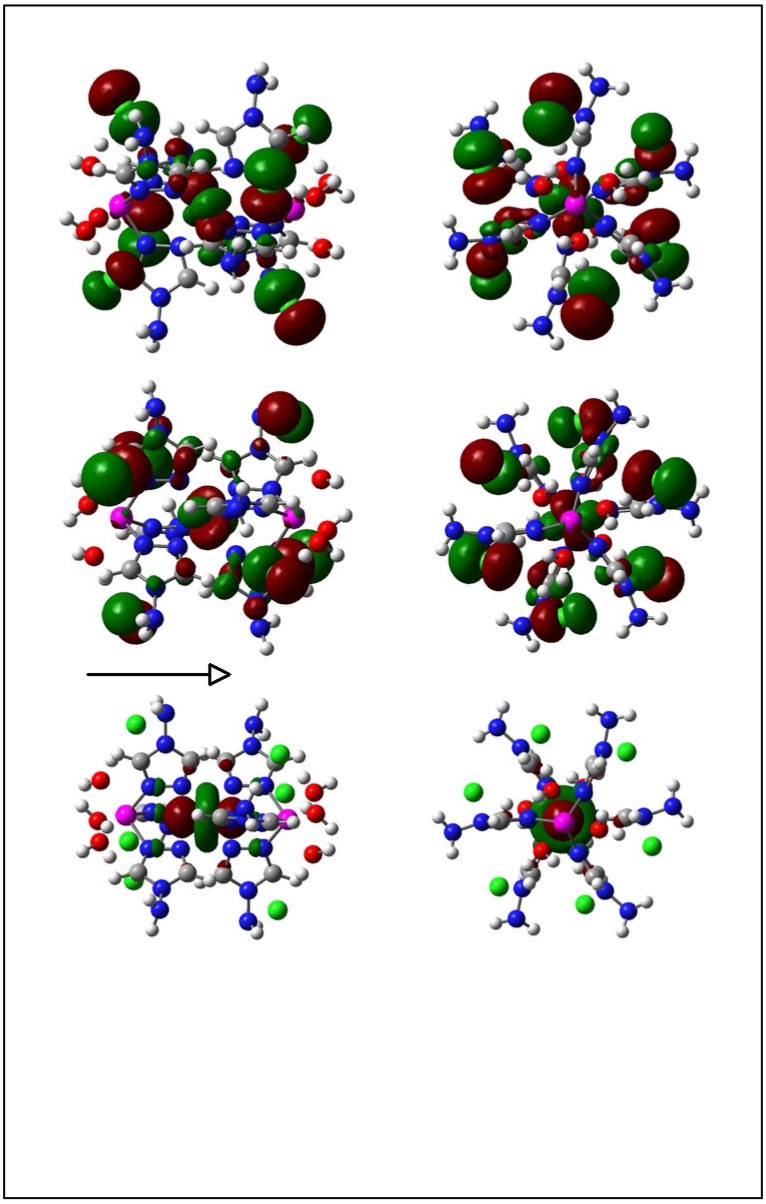

Fig. S9**:** Occupied MO orbitals (159, top, 158, middle and 141, bottom) of predominantly d-character for central Fe atom in S_6 isomer of low- spin (all three irons) of $[(H_2O)_3Fe(atrz)_3Fe(atrz)_3Fe(OH_2)_3]Cl_6$. The molecule is shown with its S_6 axis orientation given by the arrow (left) and along it, oriented perpendicularly to Figure plane (right).

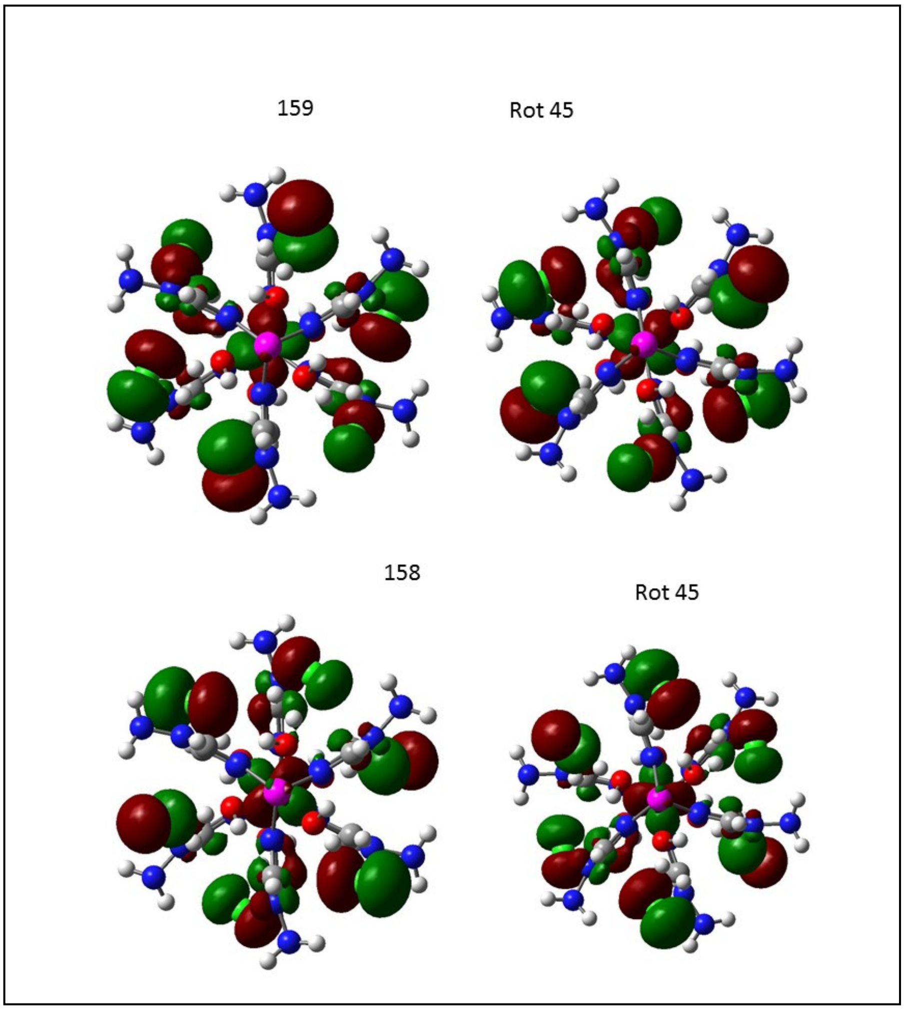

Fig. S10. Occupied orbitals 158 and 159 of $[(H_2O)_3Fe(atrz)_3Fe(atrz)_3Fe(OH_2)_3]Cl_6$ at identical orientation of the molecule (left) and after rotation at 45 deg along z-axis (long axis of the molecule)

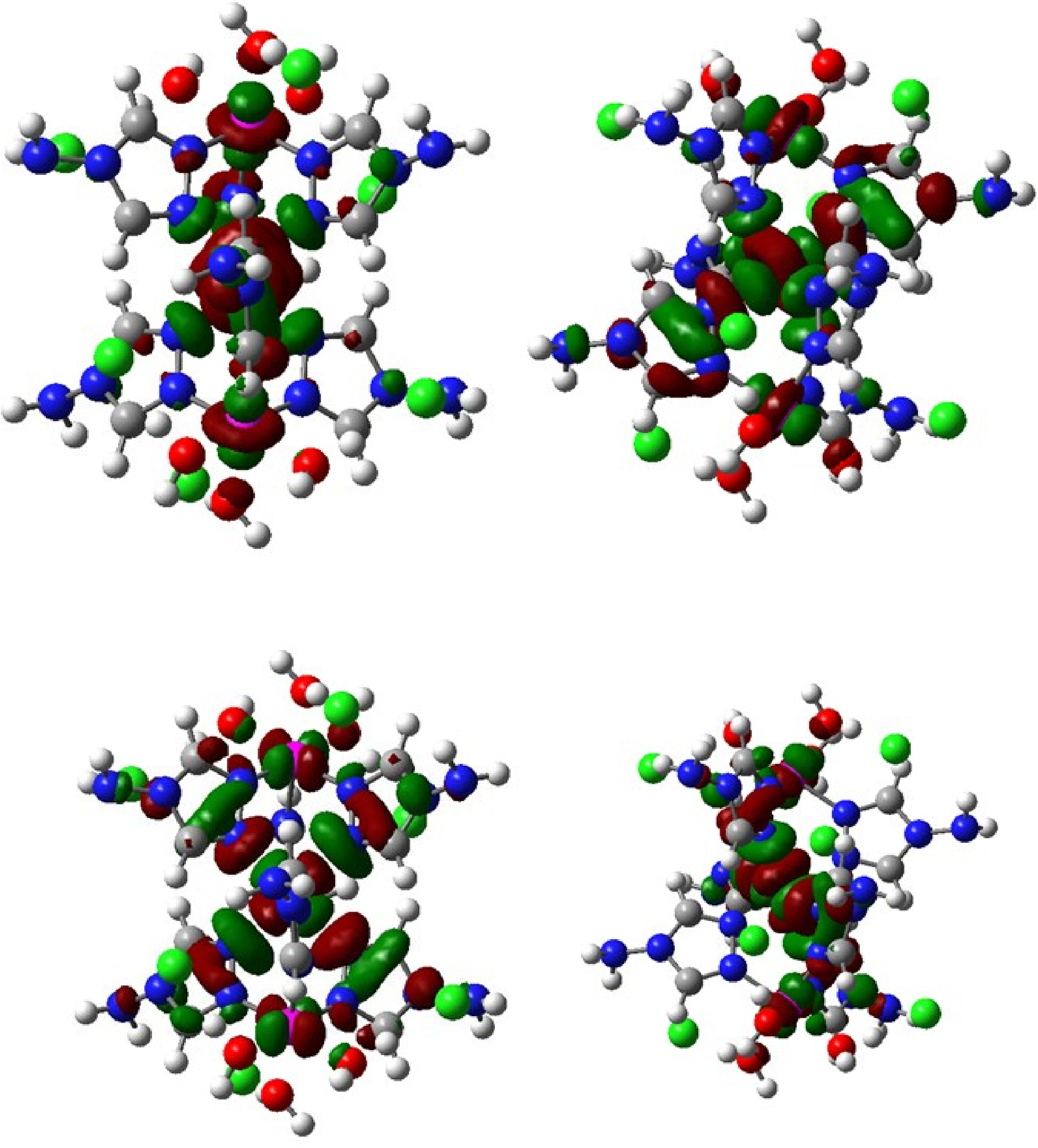

Fig. S11. Further orientation of orbitals 179 (top) and 178 (bottom) of $[(H_2O)_3Fe(atrz)_3Fe(atrz)_3Fe(OH_2)_3]Cl_6$